

# Simulation Research on the Effect of Spreading Process Parameters on the Quality of Lunar Regolith Powder Bed in Additive Manufacturing

Qi Tian, Bing Luo\*

College of Mechanical Engineering, Shenyang Ligong University, Shenyang 110159, Liaoning Province, China

\*Corresponding author: Bing Luo, [fzylingyf@163.com](mailto:fzylingyf@163.com)

**Copyright:** © 2023 Author(s). This is an open-access article distributed under the terms of the Creative Commons Attribution License (CC BY 4.0), permitting distribution and reproduction in any medium, provided the original work is cited.

**Abstract:** Lunar surface additive manufacturing with lunar regolith is a key step in *in-situ* resource utilization. The powder spreading process is the key process, which has a major impact on the quality of the powder bed and the precision of molded parts. In this study, the discrete element method (DEM) was adopted to simulate the powder spreading process with a roller. The three powder bed quality indicators, including the molding layer offset, voidage fraction, and surface roughness, were established. Besides, the influence of the three process parameters, which are roller's translational speed, rotational speed, and powder spreading layer thickness on the powder bed quality indicators was also analyzed. The results show that with the reduction of the powder spreading layer thickness and the increase of the rotational speed, the offset increased significantly; when the translational speed increased, the offset first increased and then decreased, which resulted in an extreme value; with the increase of the layer thickness and the decrease of the translational speed, the values for voidage fraction and surface roughness significantly reduced. The powder bed quality indicators were adopted as the optimization objective, and the multi-objective parameter optimization was carried out. The predicted optimal powder spreading parameters and powder bed quality indicators were then obtained. Moreover, the optimal values were then verified. This study can provide informative guidance for *in-situ* manufacturing at the moon in future deep space exploration missions.

**Keywords:** Lunar regolith additive manufacturing; Numerical simulation of powder spreading process; Discrete element method; Powder spreading process parameters; Parameters optimization

**Online publication:** May 16, 2023

## 1. Introduction

The selected laser melted (SLM) technology uses a high-energy laser beam as the heat source to irradiate the surface lunar regolith particles, and then directly melts and cools them, which turn them into parts with great performance that can be processed for different uses and has high environmental adaptability<sup>[1]</sup>. In the SLM powder spreading stage, laying a high-density powder bed with a flat surface and uniform distribution is the key to molding parts with excellent performance<sup>[2]</sup>. Therefore, it is necessary to study the forming process of the powder bed and explore the influence of the powder spreading process on the quality of the powder bed. However, due to the high cost of experiments and the fact that some micro parameters cannot be measured through experiments, the effective numerical simulation method can provide theoretical guidance and technical support for the development of the lunar regolith additive manufacturing technology.

The Discrete Element Method (DEM) has been widely used in the numerical simulation of additive

manufacturing in recent years. Wang *et al.* [3] studied the influence of the geometric shape of powder spreaders on powder spreading using DEM. Han *et al.* [4] also used DEM to study the influence of powder layer thickness on powder bed quality, which focused on analyzing the influence of powder spreading process parameters on the quality of powder bed, but did not expound on its changes in terms of specific values. Yao *et al.* [5] pointed out that the powder spreading roller may move the previous molding layer and reduce the precision of the molded part during the powder spreading process, but no further analysis was done.

Based on previous studies [3-5], DEM was adopted in this research to explore the influence of powder spreading process parameters on the quality of powder bed under a low-gravity environment. The prediction model of powder bed quality was then established, and the multi-objective optimization of powder spreading parameters was also carried out. The effectiveness of the optimization results was verified by DEM simulation. This study has certain informative and referential significance for future *in-situ* manufacturing at the moon with lunar soil as raw material.

## 2. The discrete element method model

### 2.1. Geometric model of lunar regolith particles

The shapes of lunar regolith particles are not uniform, but vary from angular, sub-angular to long strip, etc. Multi-spherical element model is used to describe particles with irregular shapes, which can simplify the interaction between particles into spherical particles, and better characterize the actual movement of particles with complex shapes. According to the SEM image of lunar regolith simulants (**Figure 1**) [6], four different shapes of lunar regolith particle models were constructed using the concept of the multi-spherical element model, as shown in **Figure 2**. These four particle models with different shapes were all superposed by spherical particles. Each shape had a main sphere and several auxiliary spheres of different sizes. Overlapping between spherical units was allowed without considering the contact force. The position, number, and size of the auxiliary spheres were determined by the actual lunar soil particles [1].

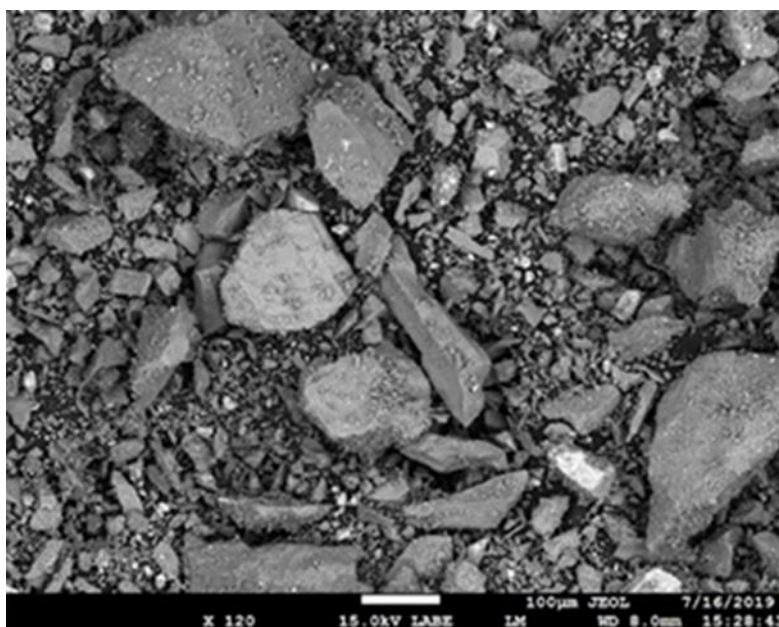


**Figure 1.** SEM image of lunar regolith simulants [6]

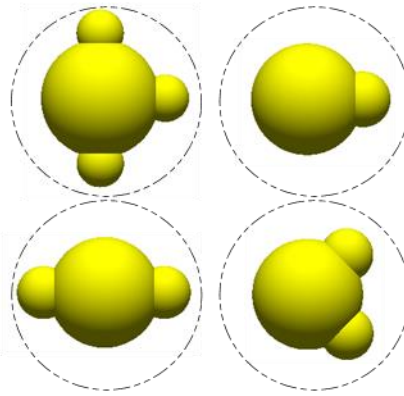


**Figure 2.** Simplified models of lunar regolith simulants

## 2.2. The discrete element method model of lunar regolith simulant

In the pre-processing of the simulation process, 4 kinds of non-spherical particle models were used to build the lunar regolith simulant, as shown in **Figure 2**. Without considering the influence of different forms of lunar regolith on powder spreading, the proportion of simulated lunar regolith particles in each form was 25%. In order to ensure the fluidity of lunar regolith particles, the generation of particles should be controlled within the range of 70-120  $\mu\text{m}$  [7]. The parameters of the lunar regolith simulant discrete element model were calibrated and checked with the static accumulation angle, as shown in **Table 1** [8-10].

**Table 1.** The DEM simulation parameters of lunar regolith

Parameter	Particle density, $\rho/(\text{kg}/\text{m}^3)$	Particle diameter, $D/(\mu\text{m})$	Poisson's ratio, $\nu$	Young's modulus, $E/(\text{MPa})$	Restitution coefficient, $\varepsilon$	Static friction coefficient, $\mu_s$	Rolling friction coefficient, $\mu_r$
Value	3350	70-120	0.47	10.3	0.5	0.5	0.16

## 2.3. The discrete element method model of powder spreading simulation

The roller type powder spreading device can not only scrape the powder bed, but also compact the powder bed through rotary movement. Therefore, the powder spreading device of the powder spreading roller was used as the research object, and a simplified model of a powder spreading roller was created, which consisted of a molding bin and powder storage bin, as shown in **Figure 3**. The powder particles were stacked in the powder storage bin, and were flattened in the forming bin by the powder spreading roller. The thickness of powder spreading can be adjusted by adjusting the height of the molding bin.

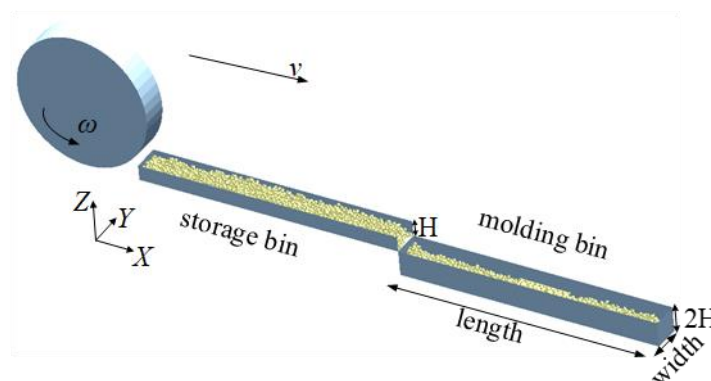


**Figure 3.** DEM model for powder spreading simulation

To improve the calculation efficiency, periodic boundary conditions were set on both sides of the Y-axis and the powder spreading device was simplified. The main characteristics of the powder spreading device were as follows: the diameter of the powder spreading roller was 2.5 mm, and the length and width of both the forming bin and the powder storage bin were 5 mm and 0.5 mm respectively. The height of the powder storage bin was consistent with the thickness of the powder spreading layer, while the height of the molding bin was twice the thickness of the powder spreading layer. Before the powder spreading by the powder spreading roller, a layer of powder particles was poured into the molding bin to create the molding layer, and the influence of the powder spreading parameters on the previous molding layer offset was studied. The powder spreading roller was tangent to the bottom of the powder storage bin and the top of the molding bin. It rotated counterclockwise, and moved forward in a straight line along the X-axis direction to completely push the particles generated in the powder storage bin to the molding bin.

### 3. Evaluation index and numerical simulation method

#### 3.1. Quality evaluation index of powder bed

The quality of the powder bed was evaluated quantitatively by two indicators - voidage fraction and surface roughness. A high-quality powder bed should have small surface roughness and voidage fraction. The quality of the parts created depends on the quality of the powder bed. This paper proposes a new index to evaluate the powder spreading process—the offset of the previous molding layer. The smaller the offset is, the higher the quality of the molded part is.

The ratio between the void volume between particles and the volume of the powder bed (stacking volume) is called the voidage fraction, and the size of the voidage fraction reflects the compactness of the particles in the powder bed. The mathematical expression of voidage fraction ( $\varphi$ ) is as follows:

$$\varphi = \sum_{i=1}^N \frac{1 - V_i}{V} \quad (1)$$

where  $V_i$  is the volume of the  $i$ -th particle;  $V$  is the total volume.

The surface roughness of the powder bed reflects the flatness of the powder layer, which greatly affects the precision of the molded parts. In this research, the average height ( $R_c$ ) of the irregular contour is used to quantitatively describe the surface roughness of the powder bed, and the average height difference between the five highest points and five lowest points of the surface particles on the powder bed is used to calculate the  $R_c$ , as shown in the formula below:

$$R_c = \frac{1}{5} \sum_j^5 (H_j - L_j) \quad (2)$$

where  $H_j$  and  $L_j$  represent the heights of the  $j$ -th highest point and  $j$ -th lowest point of surface particles on the powder bed respectively.

Yao *et al.* [5] pointed out that the powder spreading roller pushes the particles to spread the powder. Through the collision of and friction between particles, a pushing force will be generated on the former sintered molding layer. This force offsets the former molding layer, while the laser scanning path remains the same. Therefore, there will be an offset between different molding layers, and the size of the offset will affect the final molded part, as shown in **Figure 4**. Therefore, this research seeks to construct the first sintering molding layer, study the relationship between the offset and powder spreading process parameters, and reduce the offset as much as possible under the condition of meeting the corresponding powder

spreading requirements, so that molded parts with higher accuracy can be obtained.

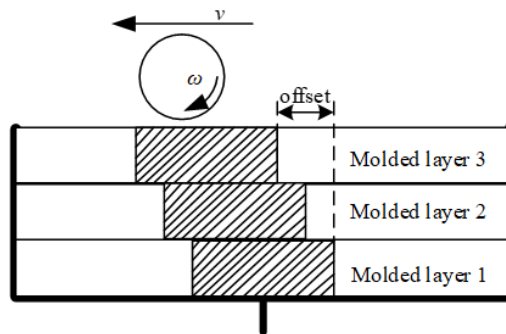


Figure 4. Model for the offset

### 3.2. The orthogonal experiment method

Three-factor and four-level orthogonal tests were designed. The factor level table is shown in **Table 2**. The powder spreading roller's translation speed ( $v$ ), rotation speed ( $\omega$ ), and powder spreading layer thickness ( $H$ ) were selected as variable factors, and 16 cases were generated using the orthogonal experiment method. The results of the response indicators are shown in **Table 3**.

Table 2. Orthogonal experiment factors and levels

Parameter	$v$ /(m/s)	$\omega$ /(rad/s)	$H$ /μm
Level 1	0.05	30	100
Level 2	0.07	60	150
Level 3	0.09	90	200
Level 4	0.11	120	250

Table 3. Orthogonal experiment design table and simulation results

Test number	Parameter			Response value		
	$v$ /(m/s)	$\omega$ /(rad/s)	$H$ /μm	$D$ /μm	$\phi$ /%	$R_c$ /μm
1	0.05	60	150	436.8	60.8	70.59
2	0.05	30	100	1216.3	73.6	131.25
3	0.07	120	200	374.2	60.6	81.53
4	0.05	90	200	194.8	58.1	48.23
5	0.11	90	150	376.7	68.9	201.29
6	0.05	120	250	61.6	57.4	46.30
7	0.11	30	250	60.1	66.1	205.56
8	0.09	120	150	483.7	66.6	96.34
9	0.09	90	100	1191.2	78.8	105.88
10	0.11	120	100	649.4	60.1	171.59
11	0.09	60	250	99.5	61.8	158.57
12	0.07	60	100	1389.2	73.0	137.37
13	0.07	90	250	144.2	58.0	92.26
14	0.07	30	150	686.6	65.1	139.88
15	0.11	60	200	175.8	68.6	175.92
16	0.09	30	200	247.3	63.6	148.65

## 4. Results and discussion

### 4.1. Regression model and analysis of variance

The data obtained in **Table 3** are fitted with multiple regression equations to obtain the regression equation, as shown in the following:

$$D = 3832.66 + 2375.296v + 3.496\omega - 34.357H - 92327.248v^2 - 0.016\omega^2 + 0.046H^2 - 79.722v\omega + 0.037\omega H + 99.887vH \quad (3)$$

$$\varphi = 94.770 + 375.956v + 0.223\omega - 0.568H - 2113.078v^2 - 0.001\omega^2 - 3.955v\omega + 0.002\omega H + 2.444vH \quad (4)$$

$$R_c = 280.093 + 339.544v + 3.108\omega - 1.234H - 10864.883v^2 + 0.002\omega^2 + 0.002H^2 + 11.437v\omega + 0.007\omega H \quad (5)$$

The ANOVA results of the three response values are shown in **Table 4**. The F values of the three models are far greater than the critical value, indicating that the three models are significant, and the predicted values are greater than 0.8, indicating that the three models have good prediction ability.

**Table 4.** Variance analysis of regression models

Response value	F	Predicted R <sup>2</sup> value	Critical F
<i>D</i>	295.9	0.969	F (0.05,12) =3.49
$\varphi$	4355.9	0.894	
<i>R<sub>c</sub></i>	525.4	0.943	

### 4.2. Impact process analysis

As shown in **Table 5**, through range analysis, *v* has the most influence on *R<sub>c</sub>* is the largest, and *H* has the most influence on *D* and  $\varphi$ , while the influence of  $\omega$  is small. As shown in **Figure 5**, within the designed range in **Table 2**, the offset increased significantly with the decrease of powder layer thickness and the increase of rotation speed; when translation speed increased, the offset first increased and then decreased, which resulted in an extreme value.

**Table 5.** Analysis of range table

Range value	<i>D</i>	$\varphi$	<i>R<sub>c</sub></i>
R1	161.875	5.15	114.4225
R2	133.35	5.85	57.395
R3	1020.175	12.475	22.94

Note: R1, R2, and R3 in the table are the range values representing translation speed, rotation speed, and powder layer thickness, respectively.

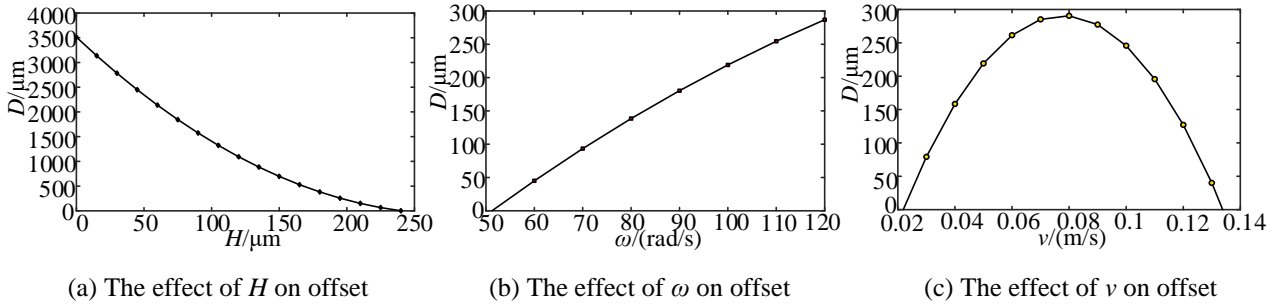


**Figure 5.** The effect of powder spreading parameters on offset ( $v = 0.05\text{m/s}$ ,  $\omega = 100\text{rad/s}$ ,  $H = 200\mu\text{m}$ )

When the thickness of the powder spreading layer decreases, the powder spreading roller will push the particles, and the energy consumed by the upper and lower particles will be reduced. The molding layer will receive greater force, and the offset will increase. The rotation of the powder spreading roller has an upward shearing effect on the powder pile. At the same time, there is particle convection in the powder pile. The particles circulate internally while moving forward. The velocity distribution is relatively dispersed, which prevents the particles from entering the powder spreading gap to form a powder spreading layer. The particles tend to move forward in the shape of a throwing line. The powder spreading layer can be formed only when moving a long distance near the base. In this process, due to the continuous collision between the upper and lower layers of particles, a lateral propulsion force is generated on the molding layer. When the rotation speed increases, the particles will move forward further, and the propulsion force on the molding layer will act for a longer time, increasing the offset. When the translation speed increases, the energy transmitted by the powder spreading roller to the particles increases, the force on the forming layer also increases, resulting in greater offset. When an extreme value is reached, the initial kinetic energy obtained by the particles still increases with the increase of the translation speed of the powder spreading roller. Besides, the horizontal displacement of particles moving in a parabolic shape also increases, and the number of particles acting on the forming layer decreases, and thus the offset decreases instead.

The influence of  $vH$  on the powder bed quality when  $\omega = 100\text{ rad/s}$  is shown in **Figure 6**. With the increase of the powder layer thickness and the decrease of the translation speed, the voidage fraction and the surface roughness decrease significantly. The particles were sheared by the powder spreading roller. When the speed increased, the shearing effect increased. When the particle medium was sheared locally, more void space was must be generated to meet the flow diffusion between particles and overcome the particle interlocking. The reduction of the thickness of the powder layer will prevent particles from passing through the gap, resulting in the reduction of the number of stacked particles and the increase of the voidage fraction. The quality of the powder bed increased with the increase of  $H$  and the decrease of  $v$ , which was consistent with the results of a research by Haeri <sup>[11]</sup>, confirming the reliability of the results of this research.

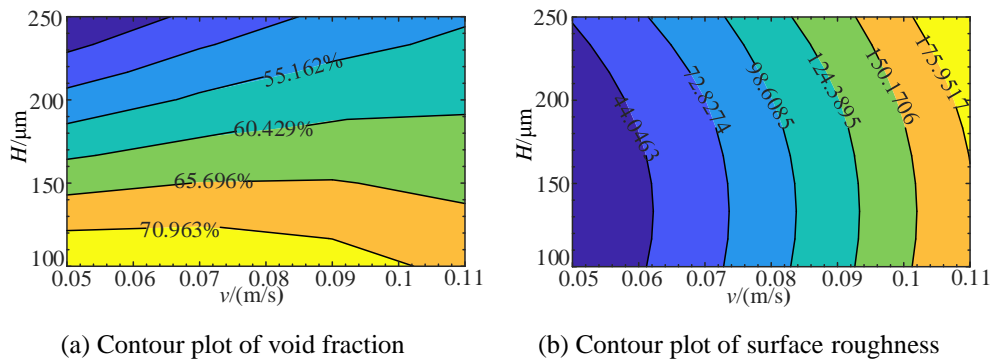


**Figure 6.** Interaction effect of V-H on powder quality indicators ( $\omega = 100\text{ rad/s}$ )

### 4.3. Multi-objective optimization

The process of powder spreading is complex, and it is difficult to build a realistic experimental environment. Therefore, it is necessary to obtain the optimal combination of powder spreading parameters through relevant optimization methods, which are defined as follows:

$$\begin{cases} \min F_{obj}(v, \omega, H) = \min(D, \varphi, R_c) \\ 0.05 \leq v \leq 0.11 \\ 30 \leq \omega \leq 120 \\ 100 \leq H \leq 250 \end{cases} \quad (6)$$

The values of the parameters were all within the range shown in **Table 2**, and the weights of the three indicators were the same. The values of relevant variables in MATLAB were defined and further optimized with genetic algorithms to obtain the optimal process parameters and response index solution set:  $v = 0.051$  m/s,  $\omega = 111$  rad/s,  $H = 231$   $\mu\text{m}$ ;  $D = 96.90$   $\mu\text{m}$ ,  $\varphi = 47.36$  %,  $R_c = 37.03$   $\mu\text{m}$ .

To verify the feasibility of the optimization results, the simulation experiments of each index were repeated three times, and the average values were taken as the final result, which were compared with the prediction results (**Table 6**). Comparing the results obtained with the results of these papers <sup>[1,12]</sup>, the error is within a reasonable range, indicating that the prediction model established is reliable.

**Table 6.** Analysis of range table

Response value	$D/\mu\text{m}$	$\varphi/\%$	$R_c/\mu\text{m}$
Predicted value	96.90	47.36	37.03
Simulation value	104.2	51.54	34.37
Error/%	7.53	8.82	7.18

### 5. Conclusion

In this paper, the influence of spreading process parameters under low gravity on the quality of powder bed is analyzed using DEM, and the process parameters were optimized using genetic algorithms to meet the requirements of additive manufacturing in the lunar environment.

- (1) The regression model of three powder bed quality indexes was established. Based on the analysis of variance, the three models can be utilized to predict and optimize the powder spreading.
- (2) The translation speed ( $v$ ) had the greatest influence on the surface roughness ( $R_c$ ), and powder spreading layer thickness ( $H$ ) had the greatest influence on the offset ( $D$ ) and the voidage fraction ( $\varphi$ ), while rotation speed ( $\omega$ ) has the least influence. For the index of offset, the offset increased significantly with the decrease of powder layer thickness and the increase of rotation speed. When translation speed increased, the offset first increased and then decreased, which resulted in an extreme value.
- (3) With optimizing the powder bed quality as the objective, the multi-objective optimization of the powder spreading process parameters was carried out, and the predicted results were in good agreement with the simulation results. The optimal process parameters were determined as follows:  $v = 0.051$  m/s,  $\omega = 111$  rad/s,  $H = 231$   $\mu\text{m}$ .

### Disclosure statement

The authors declare no conflict of interest.

## References

- [1] Li W, Xu KN, Huang Y, et al., 2020, Numerical Simulation of Spreading Process of Lunar Regolith Simulant by DEM. *Journal of Beijing University of Aeronautics and Astronautics*, 46(10): 1863–1873.
- [2] Tan YQ, Xiao XW, Zhang JT, et al., 2019, Determination of Discrete Element Model Contact Parameters of Nylon Powder at SLS Preheating Temperature and Its Flow Characteristics. *Chinese Journal of Theoretical and Applied Mechanics*, 51(1): 56–63.
- [3] Wang L, Yu AB, Li EL, et al., 2021, Effects of Spreader Geometry on Powder Spreading Process in Powder Bed Additive Manufacturing. *Powder Technology*, 384(2): 211–222.
- [4] Han QQ, Gu H, Setchi R, 2019, Discrete Element Simulation of Powder Layer Thickness in Laser Additive Manufacturing. *Powder Technology*, 352(4): 91–102.
- [5] Yao HB, Wang C, Fan N, et al., 2020, Structural Design of Selective Laser Sintering Powder Transmission Device. *Applied Laser*, 40(1): 47–57.
- [6] Isachenkov M, Chugunov S, Akhatov I, et al., 2021, Regolith-Based Additive Manufacturing for Sustainable Development of Lunar Infrastructure: An Overview. *Acta Astronautica*, 180: 650–678.
- [7] Li W, Xu KN, Huang Y, et al., 2019, In-Situ Forming of Lunar Regolith Simulant via Selective Laser Melting. *Journal of Beijing University of Aeronautics and Astronautics*, 45(10): 1931–1937.
- [8] Khalid AA, Alsidqi H, et al., 2009, Strength Properties of JSC-1A Lunar Regolith Simulant. *Journal of Geotechnical and Geo-environmental Engineering*, 135(5): 673–679.
- [9] Liang SM, Wang YB, Wang LX, et al., 2019, Landing Process of Lunar Lander Simulated with Coupled DEM-FEM Model. *Chinese Journal of Solid Mechanics*, 40(1): 39–50.
- [10] Lin CX, Ling DS, Zhong SY, et al., 2017, Experimental Research and Discrete Element Analysis of Shear Strength of Lunar Soil Simulants. *Rock and Soil Mechanics*, 38(3): 893–901.
- [11] Haeri S, Wang Y, Ghita O, et al., 2017, Discrete Element Simulation and Experimental Study of Powder Spreading Process in Additive Manufacturing. *Powder Technology*, 306: 45–54.
- [12] Zhang JT, Tan YQ, Ji CY, et al., 2021, Research on the Effects of Roller-Spreading Parameters for Nylon Powder Spreadability in Additive Manufacturing. *Chinese Journal of Theoretical and Applied Mechanics*, 53(9): 2416–2426.

### Publisher's note

Bio-Byword Scientific Publishing remains neutral with regard to jurisdictional claims in published maps and institutional affiliations.